

Other emerging dAFM techniques

Slide Switch ~ 46:00

- Multi-frequency AFM
- Sub-surface imaging
- High-speed/video rate AFM

Start ~ 50:30

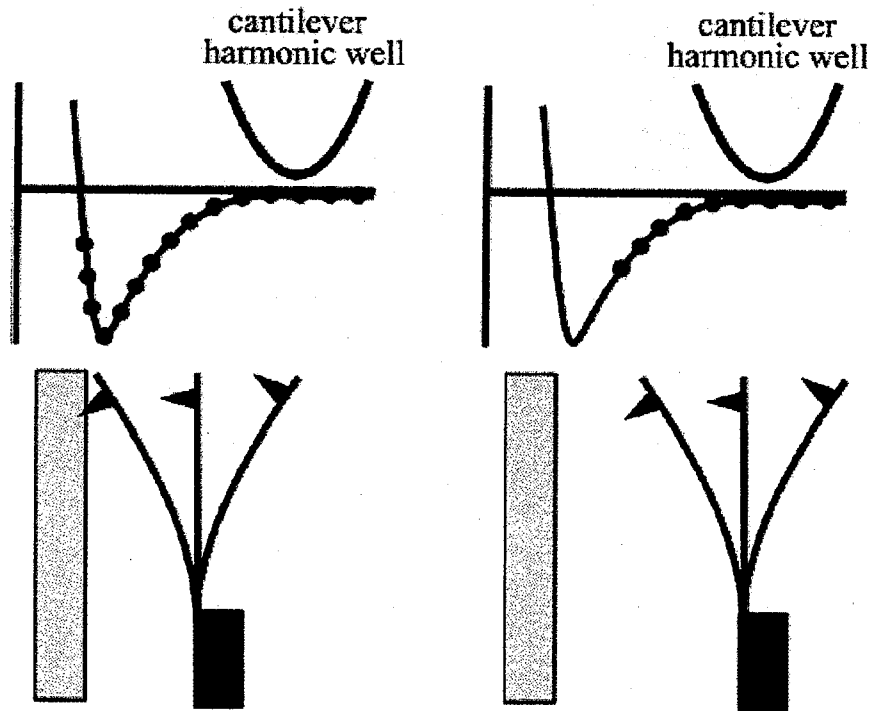
LL

Multi-frequency AFM

- Generic term applied to all methods where either cantilever is excited and or measured at more than one frequency
 - Kelvin force microscopy in tapping mode (discussed in class)
 - Higher harmonic imaging
 - Internally resonant or "harmonic" cantilevers
 - Momentary excitation in liquids
 - Bimodal or dual AC mode
 - Band excitation (Oakridge, S. Jesse, S. Kalinin)

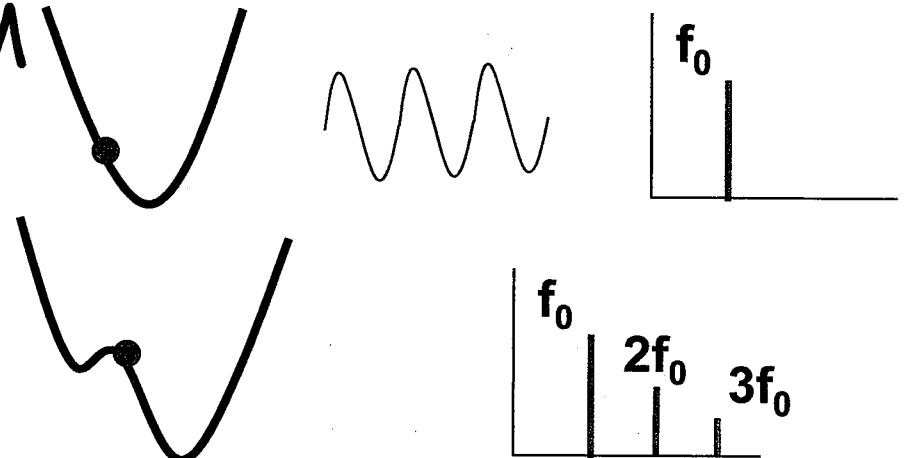
Multi-frequency AFM

- Higher harmonic dAFM
- Insight:



mechanical properties &
loss mechanisms

Hamaker constants,
electro-statics & -dynamics



U. Durig, New J. Phys., 2, 2000
M. Stark et al, PNAS, 99, 2002
Crittenden et al, PRB, 72, 2006

Multi-frequency AFM

Higher harmonic dAFM

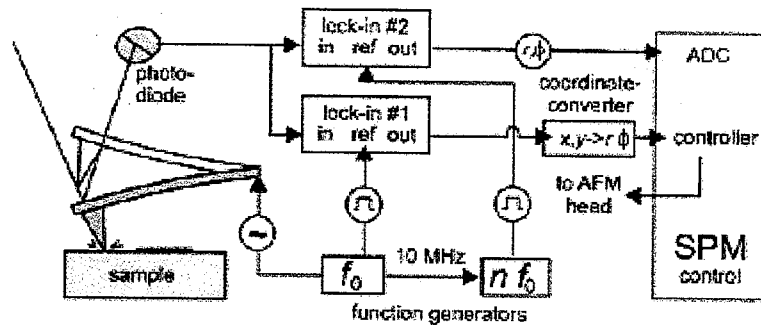


FIG. 1. Experimental setup for the detection of anharmonic signals. A commercial AFM is equipped with a second lock-in amplifier for the detection of anharmonic signals.

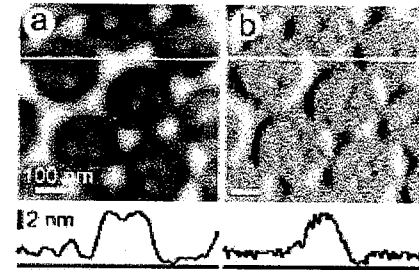


FIG. 2. (a) Topographic (b) control error, and (c)–(e) higher order harmonic images of a 4-nm-thick Pt–C test structure on a fused silica cover slip. The driving frequency was $f = 52.2$ kHz, the detection frequencies were (c) $3f = 156.6$ kHz, (d) $5f = 261.0$ kHz, and (e) $8f = 417.6$ kHz.

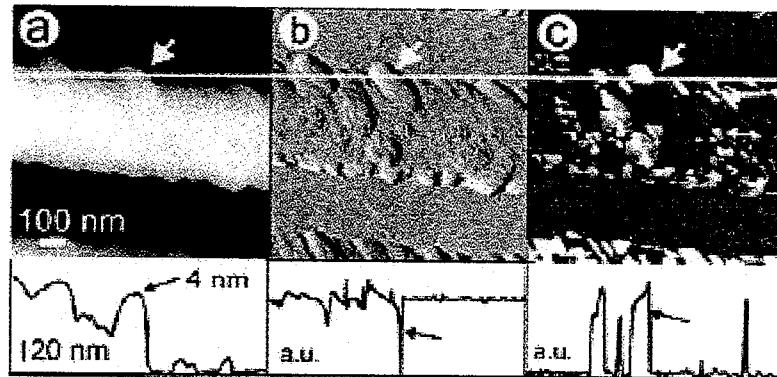


FIG. 4. Detail of a silicon test structure imaged in tapping mode (scan direction right to left). (a) Topography, (b) control error, and (c) eighth harmonic. The instabilities due to the bistable behavior of the system are difficult to be seen in the conventional images (a) and (b). However, in the harmonic image (c) a strong contrast prevails.

Amplifying higher harmonics

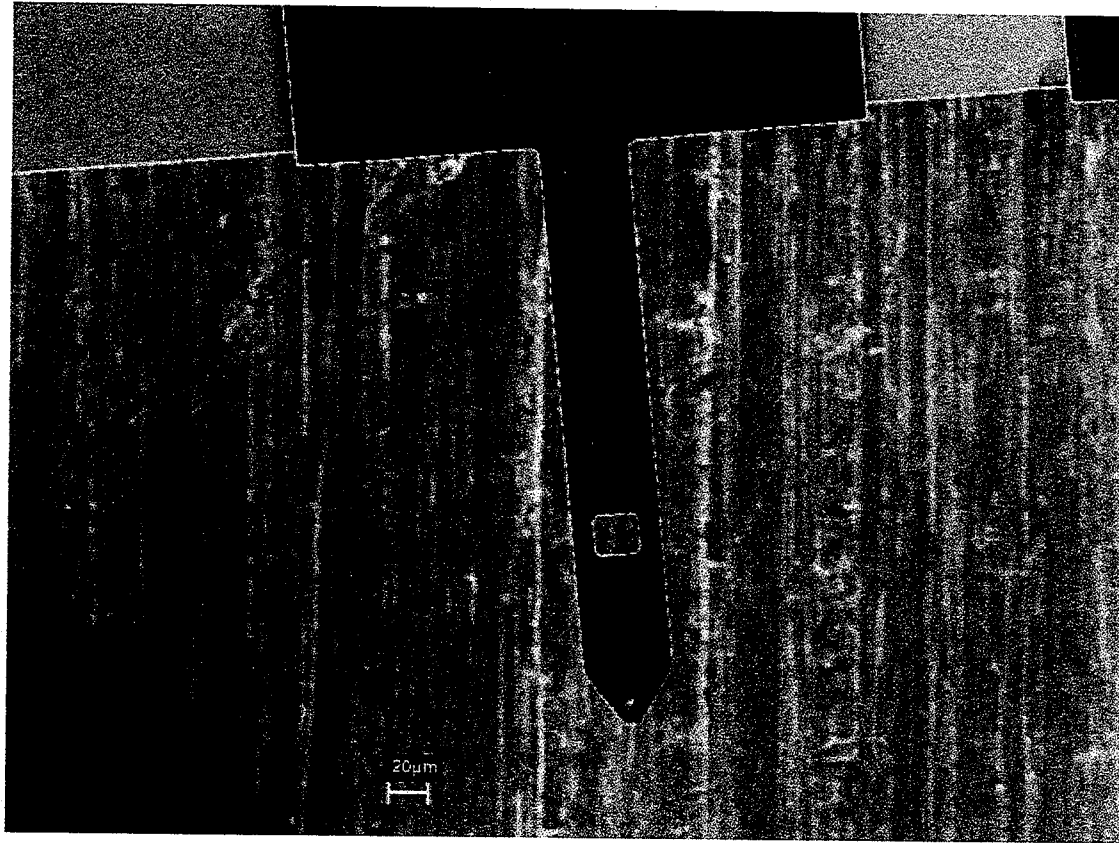
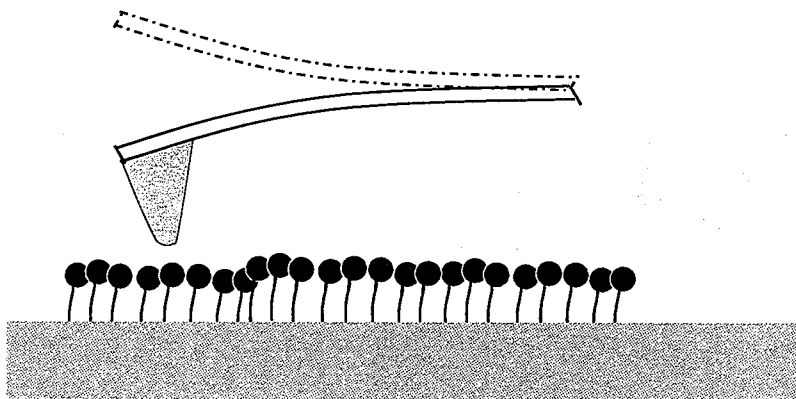


Fig. 6. SEM image of a harmonic cantilever. Width, length and thickness of the cantilever are 50, 300, and 2.2 μm , respectively. The rectangular opening is 22 μm \times 18 μm and centered 190 μm away from the cantilever base.

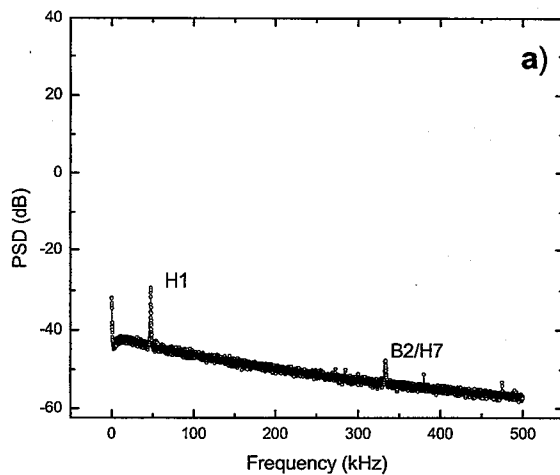
- Tune second eigenmode frequency to an integer multiple of the fundamental

Using tuned cantilevers

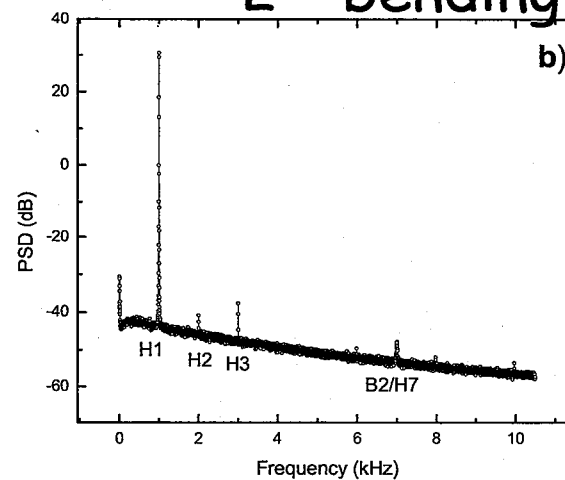
- In attractive regime, vibration spectrum depends on local vdW and electrostatic forces
- Experiments performed using 47 kHz microcantilever on wild and mutant bacteriorhodopsin membrane



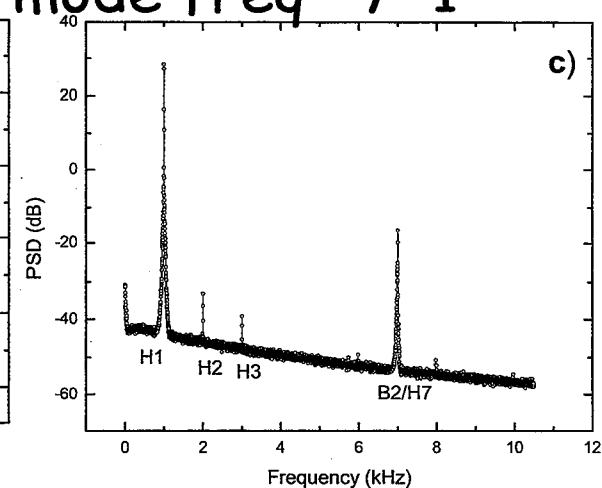
- 2nd bending mode freq $\sim 7 \times 1^{\text{st}}$



Thermal vibration



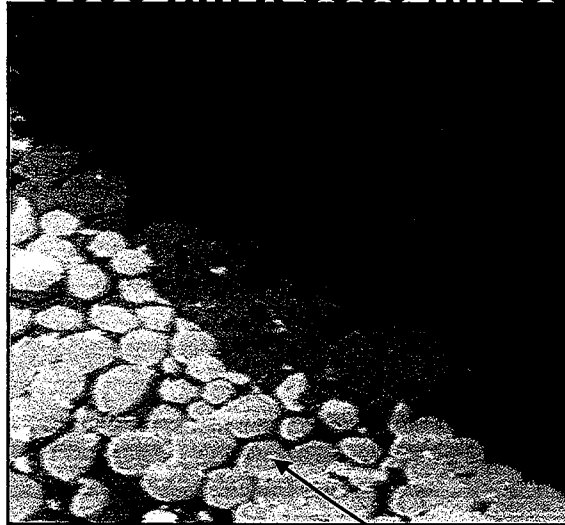
Driven in air



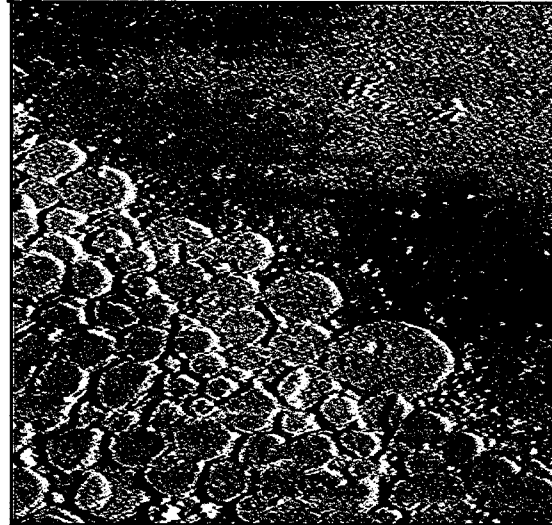
On mica (50 %
setpoint)

Using tuned cantilevers

3500 nm x 3500 nm scans



Topography



Second harmonic
image



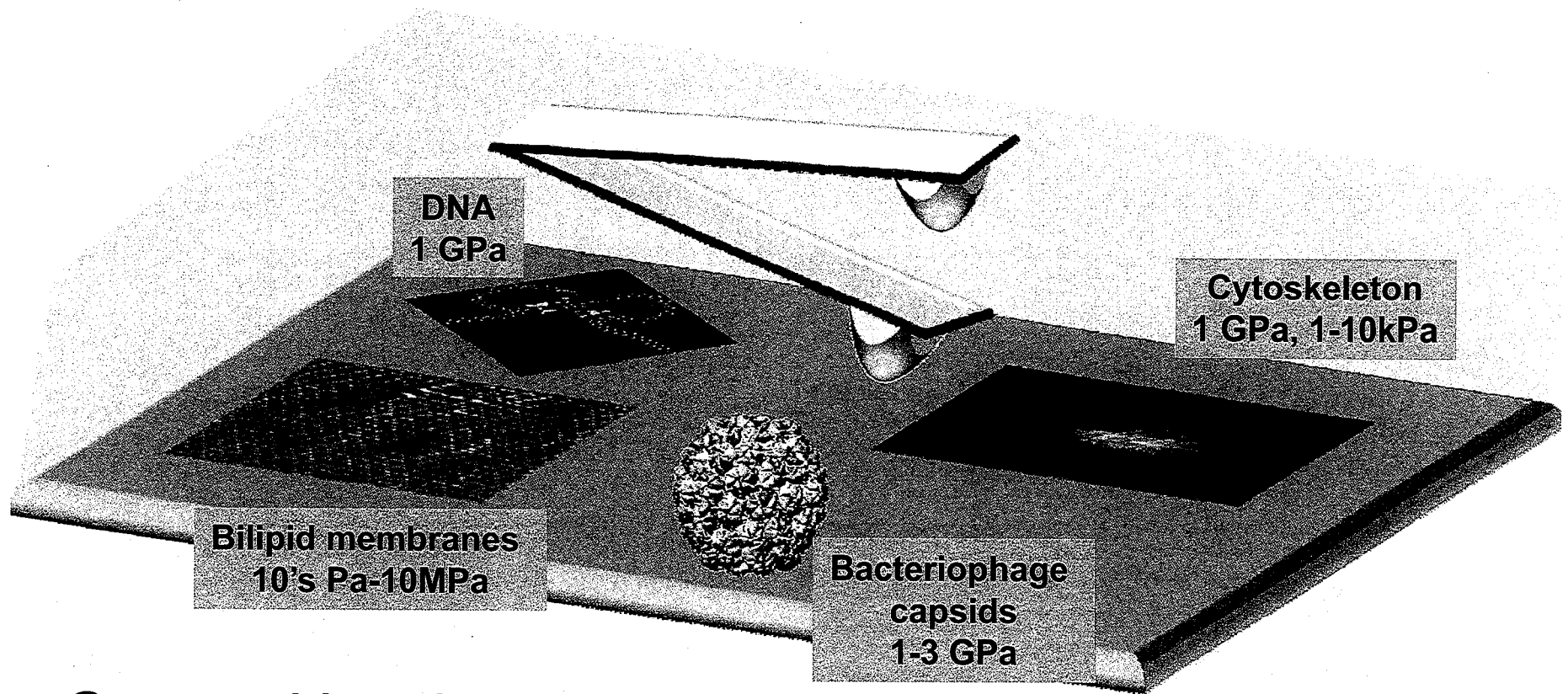
Seventh harmonic
image

proteins

Lipid deposits

- Clear distinction between lipids and proteins
- Presence of internal resonance critical in the method
- The method shows promise for the measurement of local Hamaker constants of soft biomolecules
- Can be extended to electrostatic force microscopy

Momentary excitation in liquids



Compositional contrast in liquids

- Van Noort et al, (Langmuir, 1999)
- Preiner, Hinterdorfer et al (PRL, 2007) Second harmonic
- Xu, Melcher, Raman, Reifenberger (PRL, 2009) Momentary

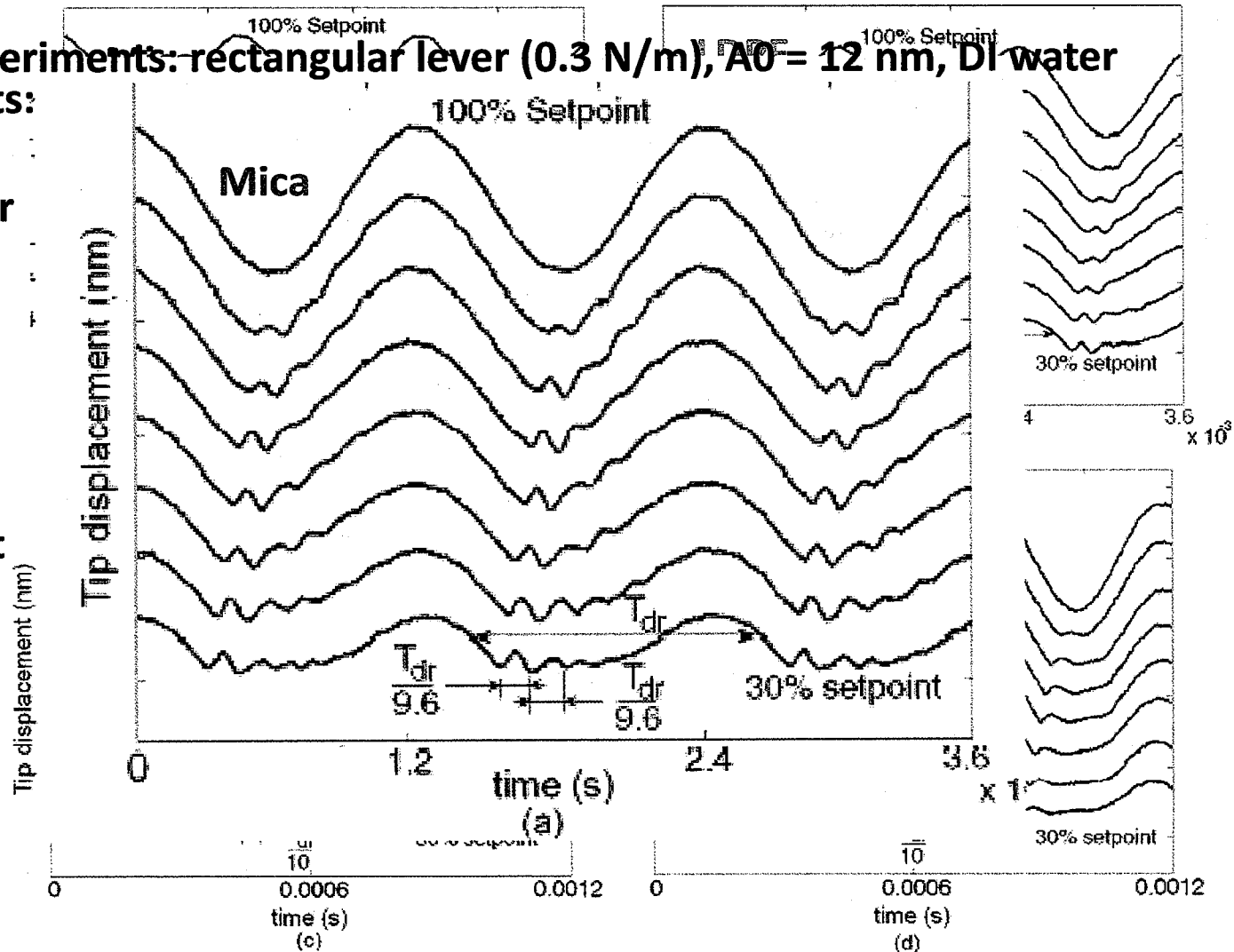
Momentary excitation - experiments

(Basak and Raman, App. Phys. Lett., 2007)

Experiments:
0.3 N/m
rectangular
lever

Experiment
s:
0.1 N/m
triangular
lever

Experiments: rectangular lever (0.3 N/m), $A_0 = 12$ nm, DI water

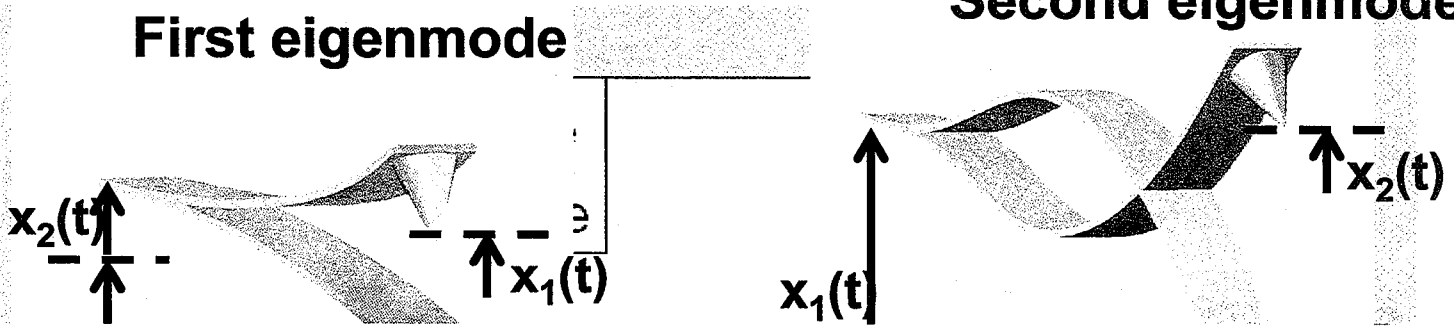


Momentary excitation- theory

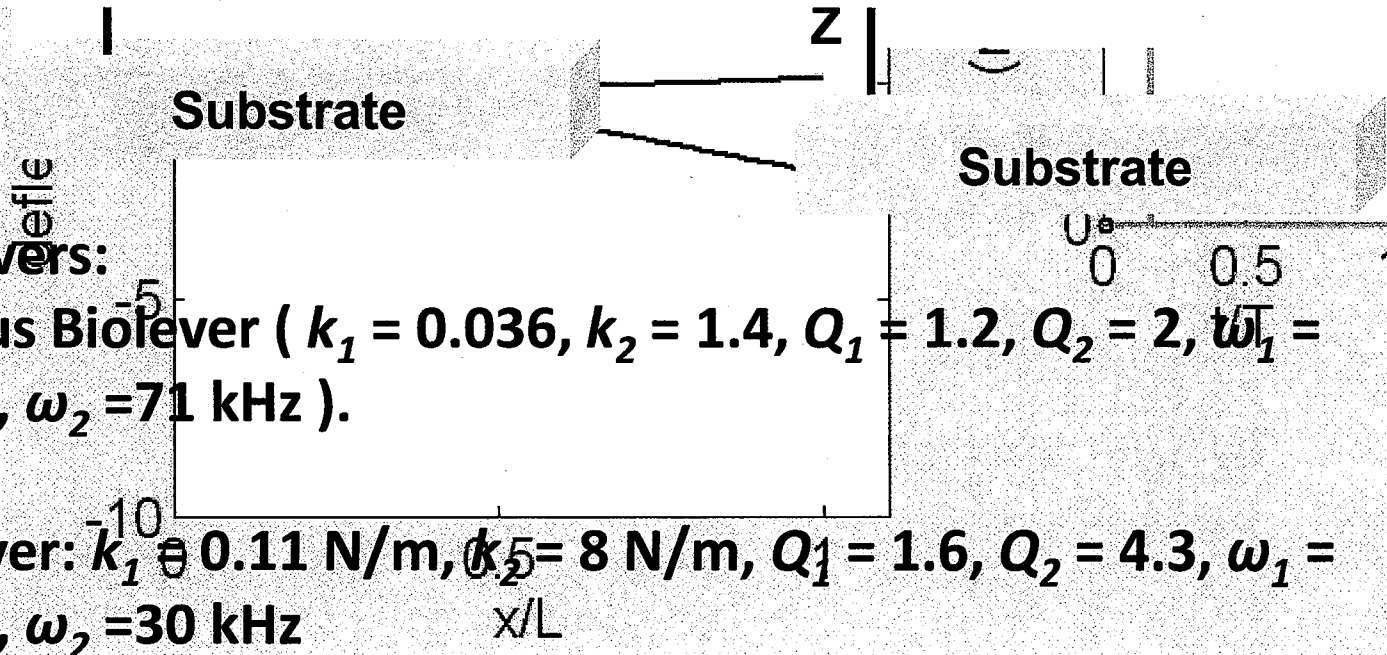
Decomposed cantilever motion $\Delta/\Delta = 0.05$

First eigenmode

Second eigenmode



- Momentary excitation is greater on stiffer samples



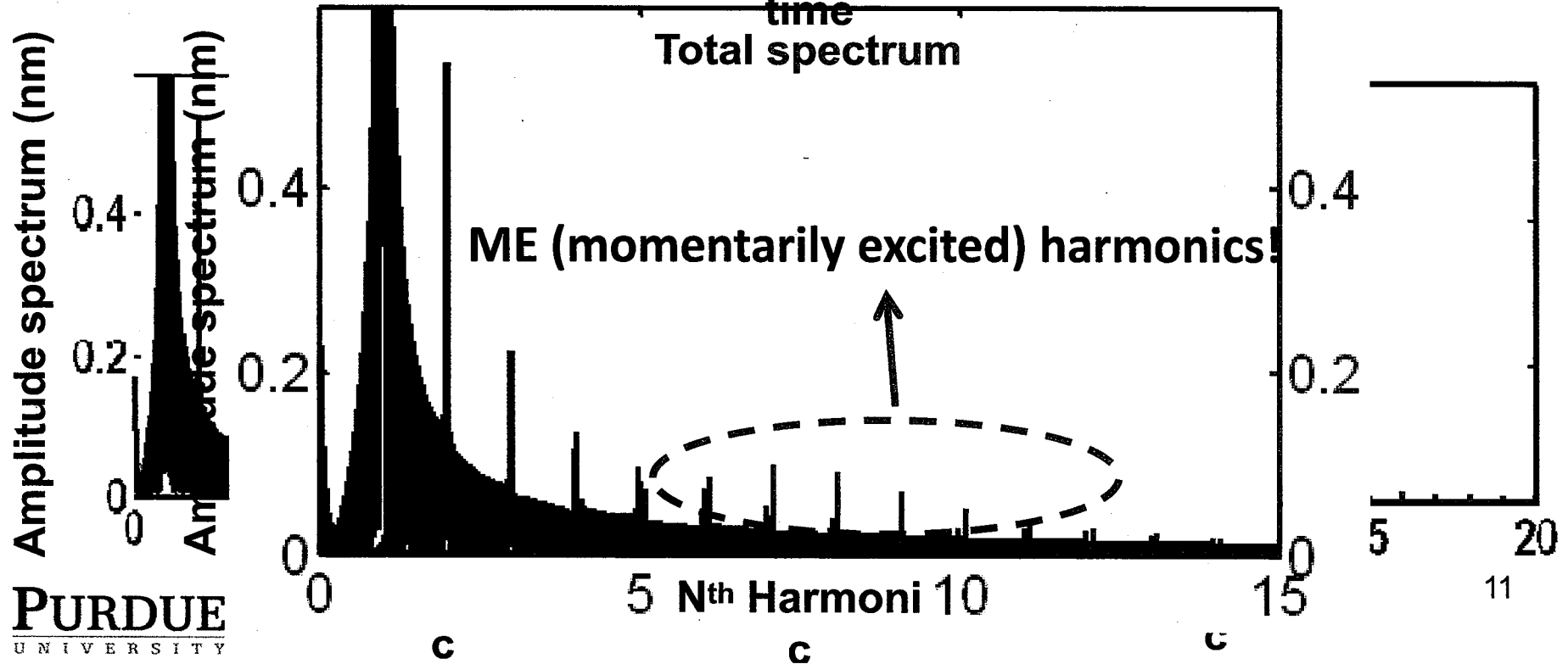
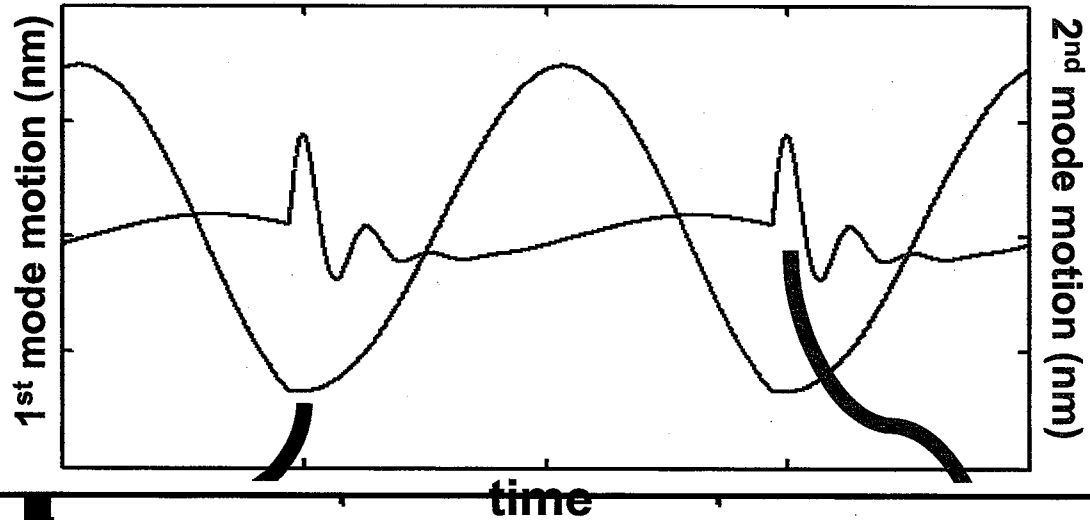
Cantilevers:

Olympus Biolever ($k_1 = 0.036$, $k_2 = 1.4$, $Q_1 = 1.2$, $Q_2 = 2$, $\omega_1 = 9.3$ kHz, $\omega_2 = 71$ kHz).

MAClever: $k_1 \approx 0.11$ N/m, $k_2 = 8$ N/m, $Q_1 = 1.6$, $Q_2 = 4.3$, $\omega_1 = 3.5$ kHz, $\omega_2 = 30$ kHz

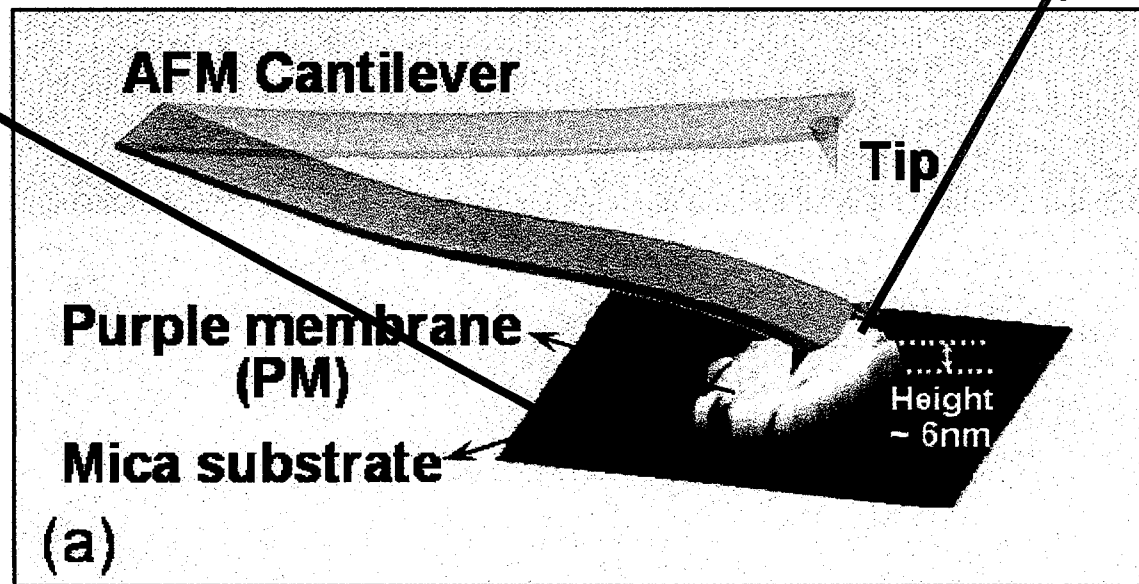
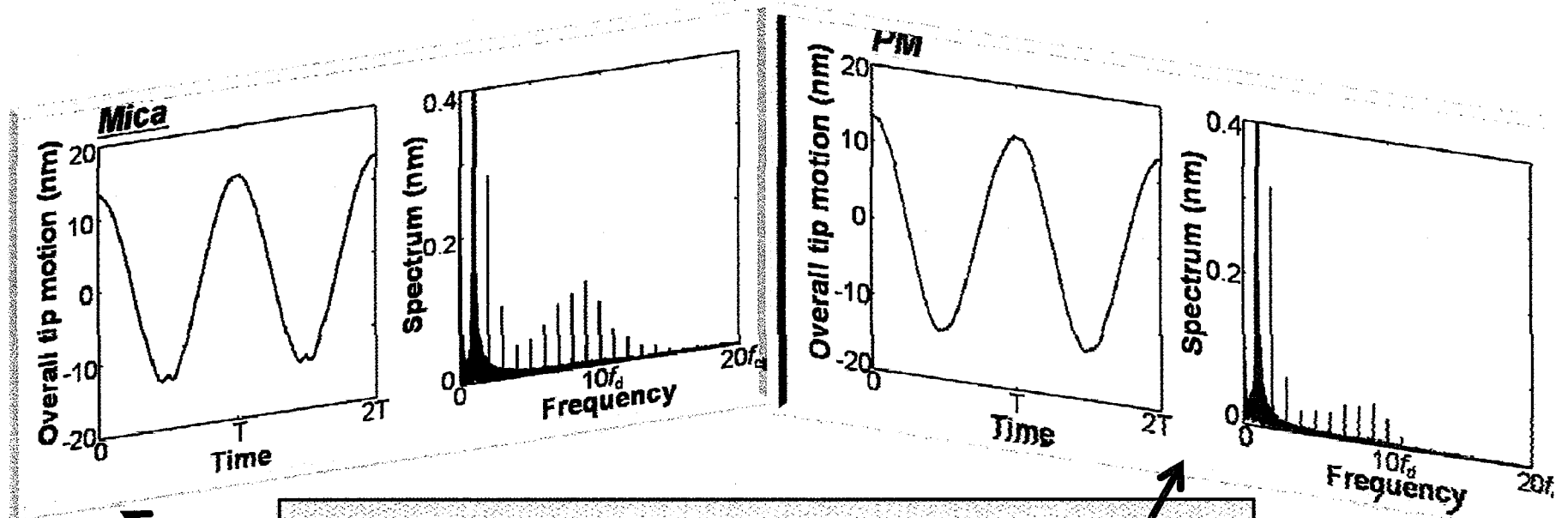
Momentarily Excited (ME) Harmonics

Simulations:
MAClever,
 $A_0=15\text{nm},$
 $A/A_0=0.92$



Application to elasticity mapping

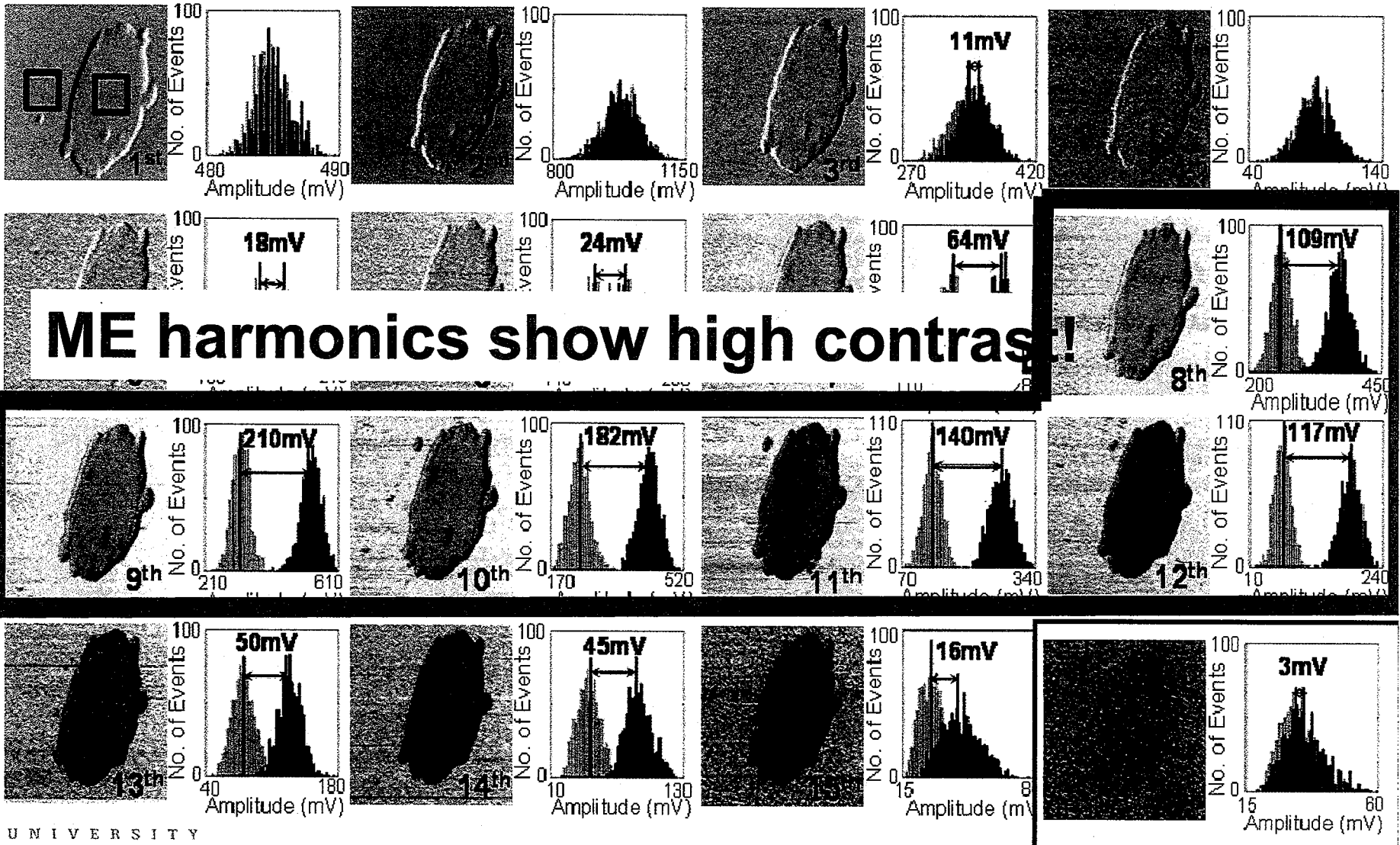
Xu et al. Phys. Rev. Lett. 2009



Higher Harmonic Imaging

Xu et al Phys. Rev. Lett. 2009

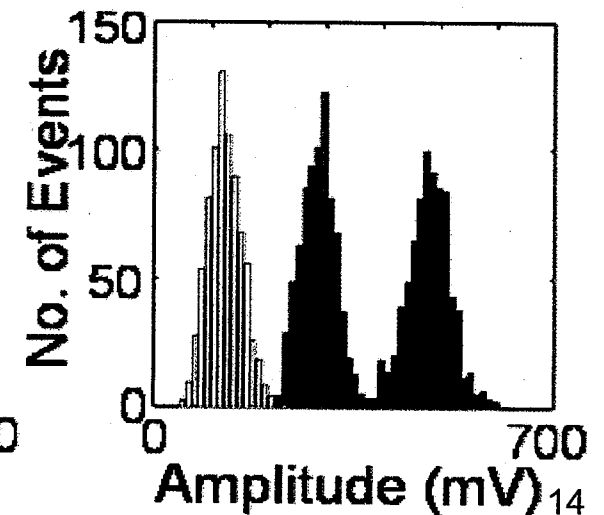
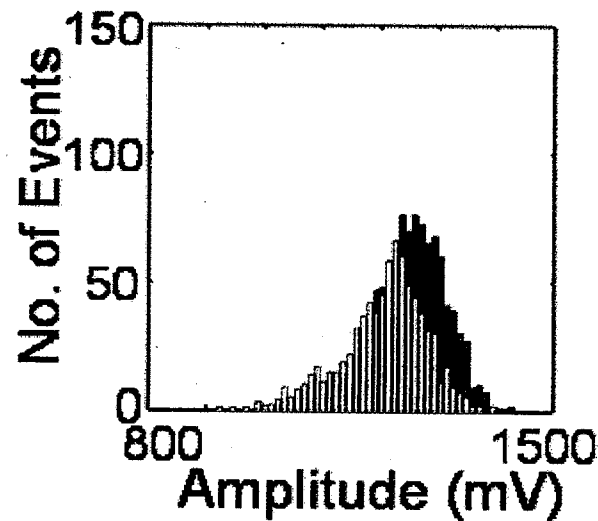
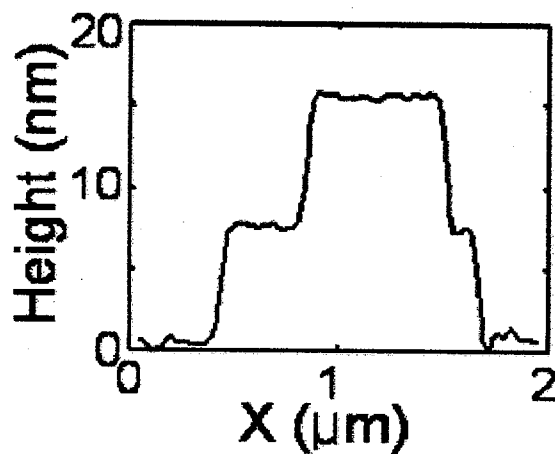
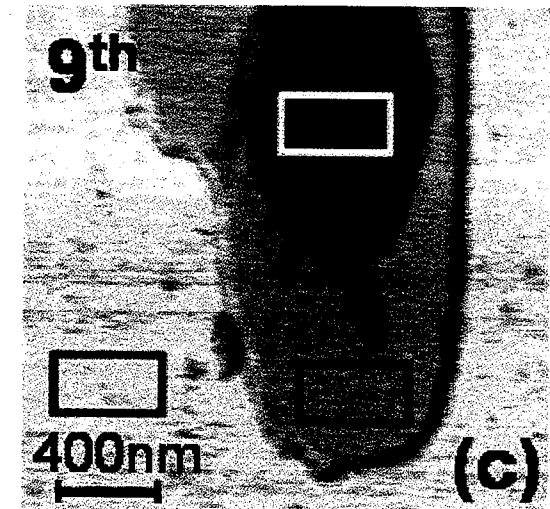
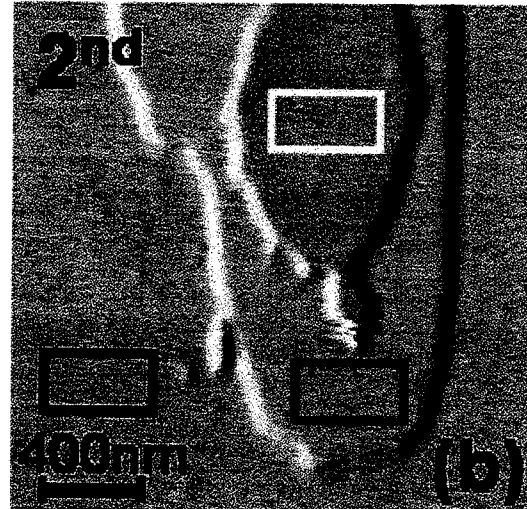
Experiment: purple membrane on mica, $k_1=0.11$ N/m, $A_0=15$ nm, A_{set}



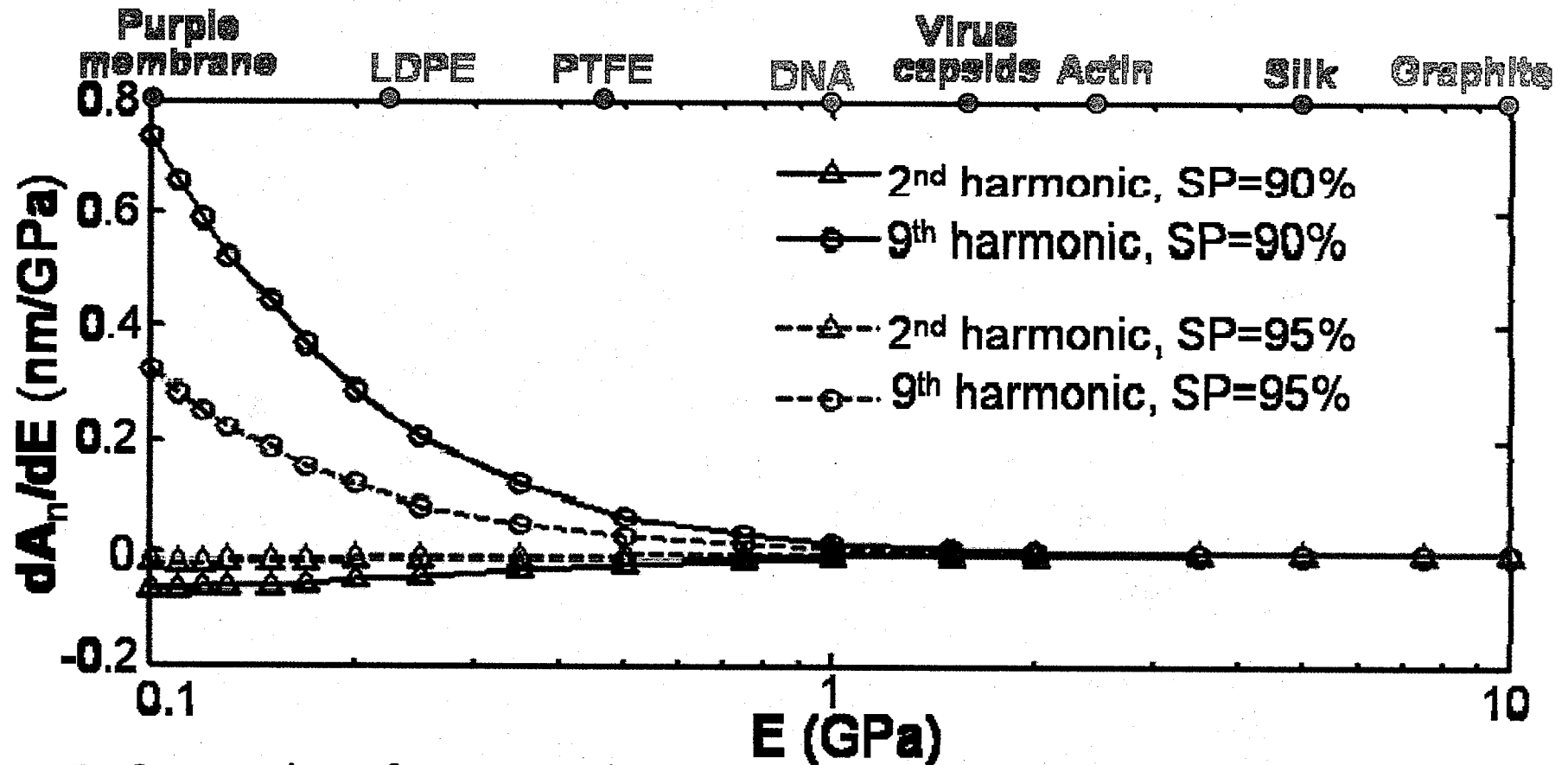
Elasticity contrast for soft samples

Xu, Melcher, Basak, Reifenberger Raman, in Phys. Rev. Lett. 2009

$k_1=0.11$ N/m, $A_0=12.5$ nm, $A_{\text{setpoint}}=92\%$, buffer: 300 mM KCl, 20 mM Tris-H



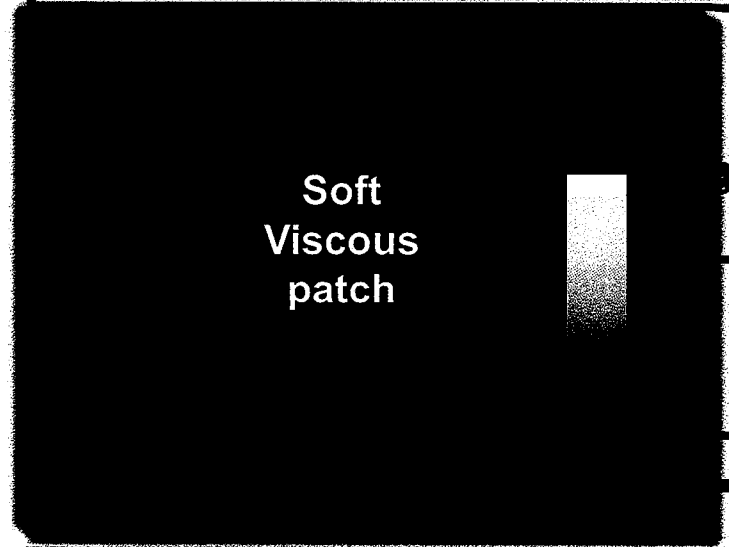
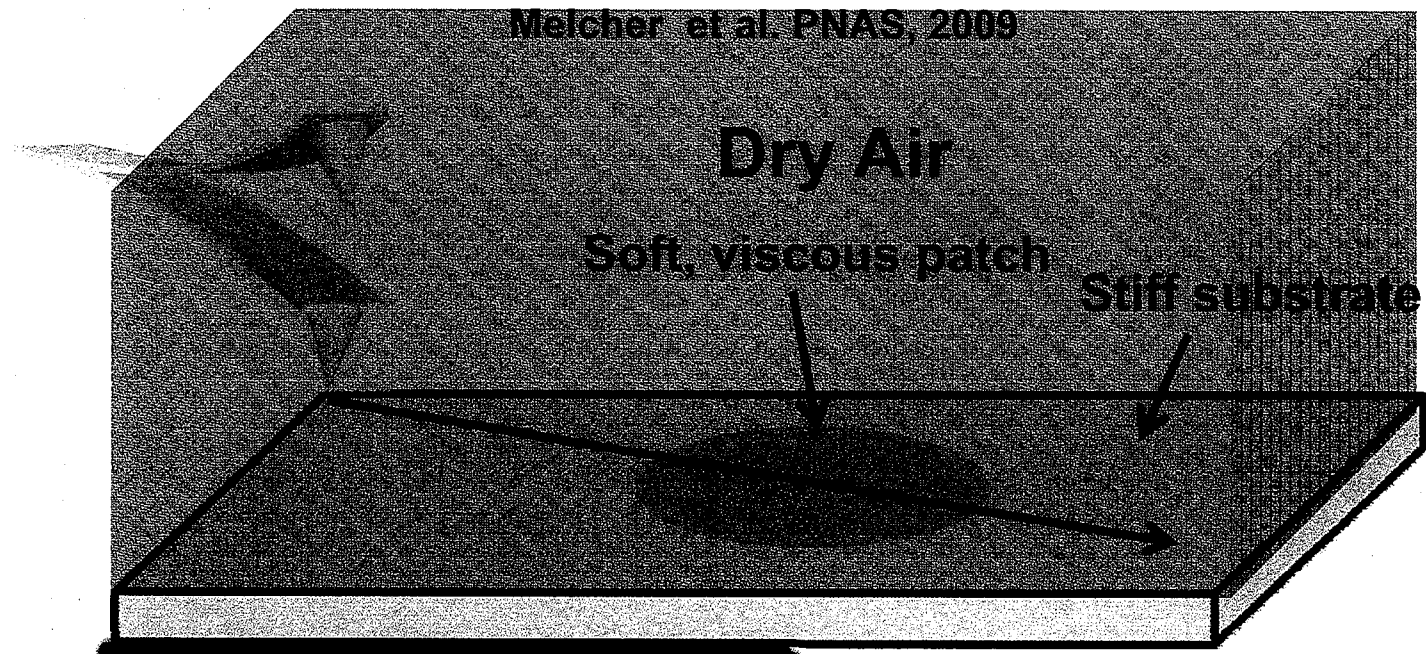
Origin of contrast in ME harmonic images



- One order of magnitude improvement in elasticity contrast using ME harmonics compared to 2nd harmonic for soft materials
- ME harmonics are closely correlated to contact time (which varies inversely with sample elasticity)

■ Image contrast seen is entirely local elasticity contrast

Phase contrast imaging in liquids

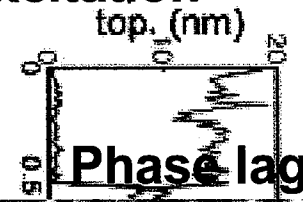
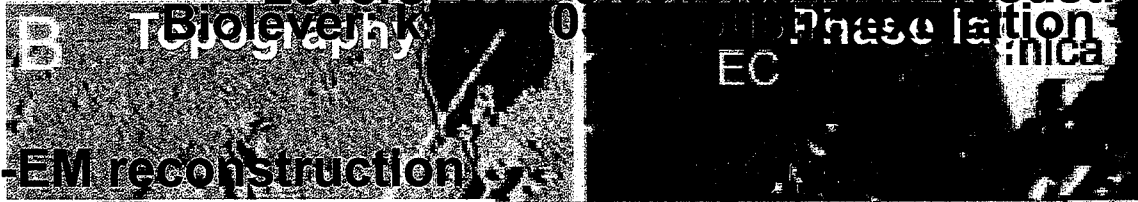


- Phase lag in Air
- Phase contrast is a measure of energy lost during interaction with the sample.
- Momentary excitation is a from of energy loss!
- Momentary excitation is larger on stiff samples

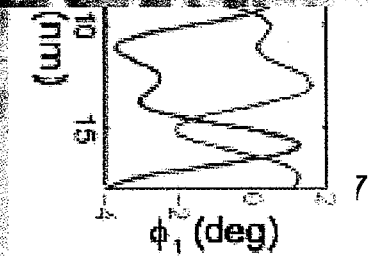
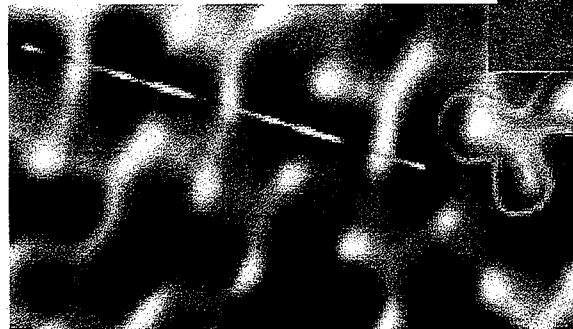
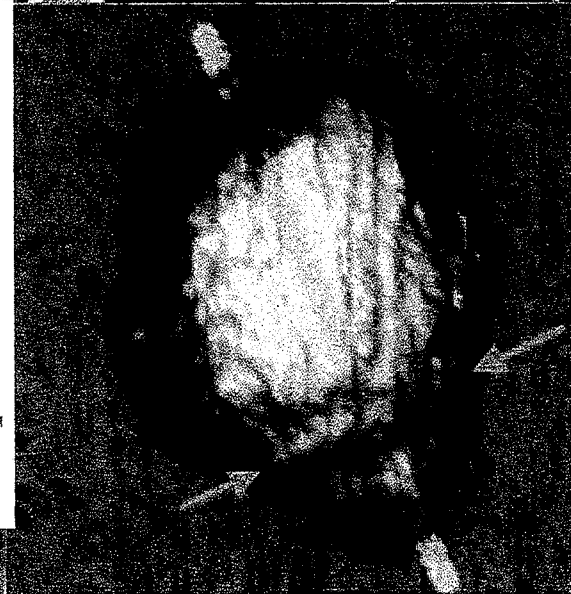
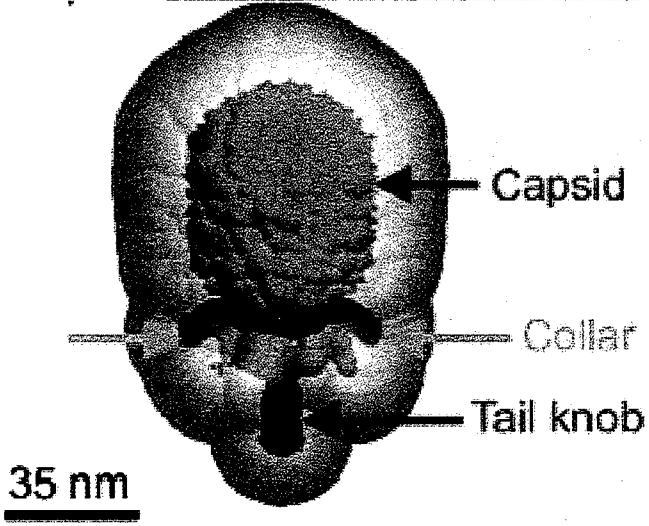
Experimental data

Melcher et al. (PNAS 2009)

Purple Membrane on mica substrate
 $\phi 29$ virus capsid on a glass substrate
 buffer solution: 300 mM KCl, 20 mM Tris-HCl, pH 7.8
 buffer: TMS pH 7.8
 Levers: $k_1 = 0.58, 0.09$ N/m, acoustic excitation

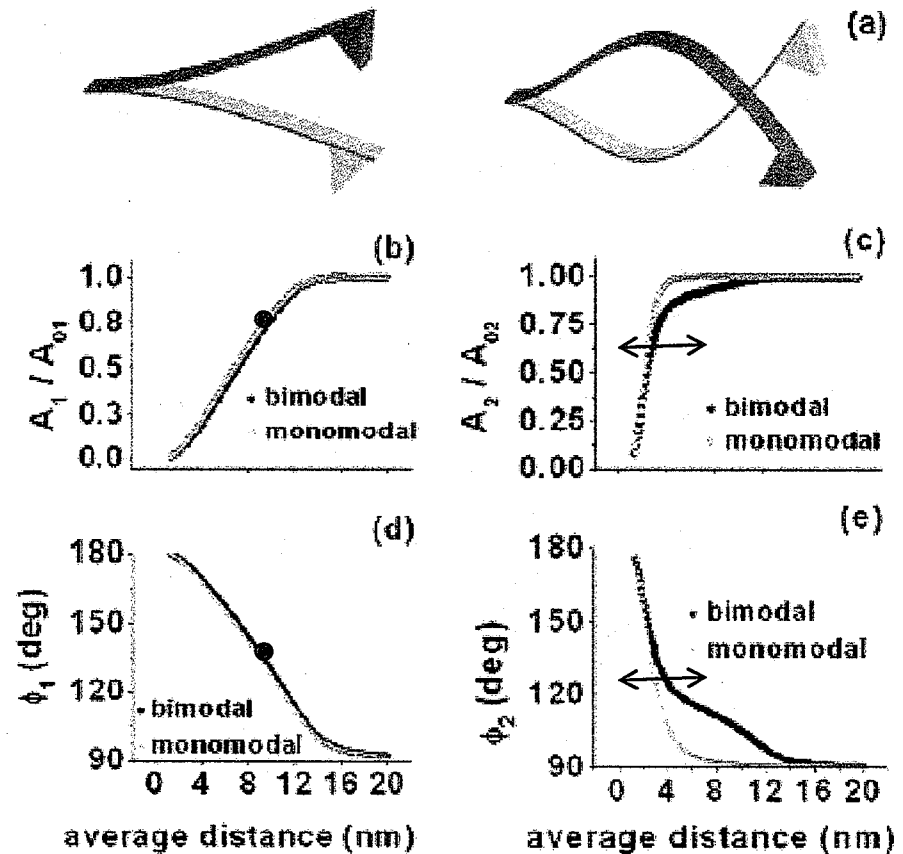


Cryo-EM reconstruction



Multi-frequency AFM

- Bimodal or dual AC
 - Key insight is that the second mode A_2 , ϕ_2 varies in time
 - Thus ϕ_2 not only measures dissipation but also conservative tip-sample interactions!
 - It becomes possible to see material contrast in the attractive regime!



Rodriguez and Garcia, APL, 84(3), 2004
 Lozano and Garcia, PRL, 100(7), 2008
 Lozano, Garcia, PRB, 79(1), 2009
 R. Proksch, APL, 89(11), 2006

Multi-frequency AFM

■ Bimodal or dual AC

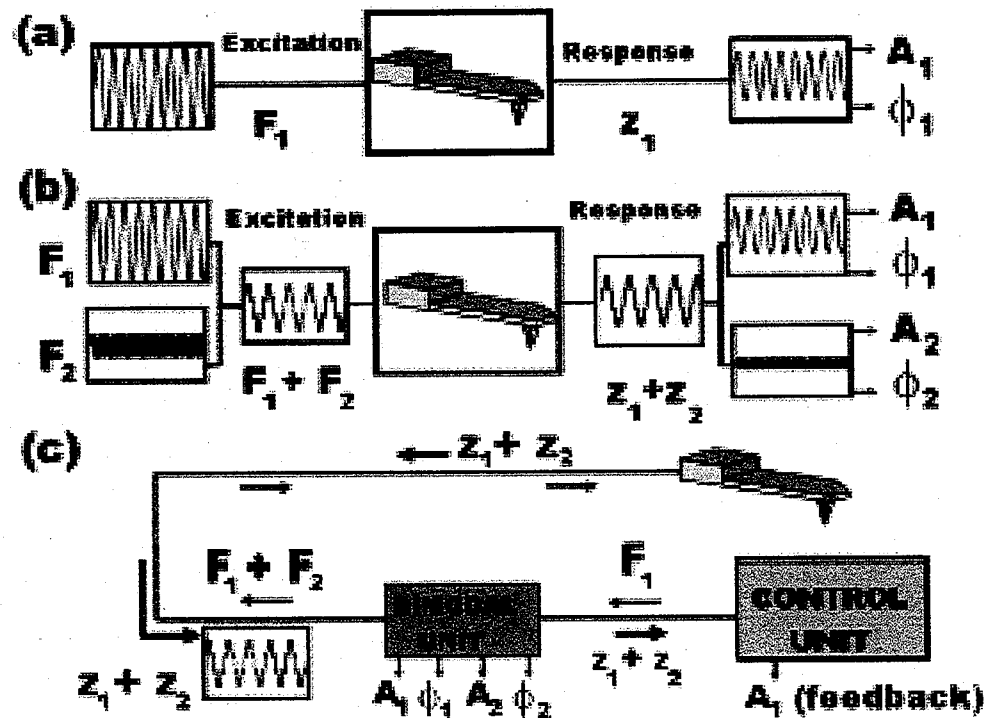


Figure 1. Comparison between amplitude modulation and bimodal AFM. (a) AM-AFM (monomodal excitation). (b) Bimodal AFM. (c) Schematics of the bimodal AFM instrument. The bimodal excitation/detection unit performs the multifrequency excitation and the multicomponent signal processing while the control unit runs the feedback.

Multi-frequency AFM

■ Bimodal or dual AC

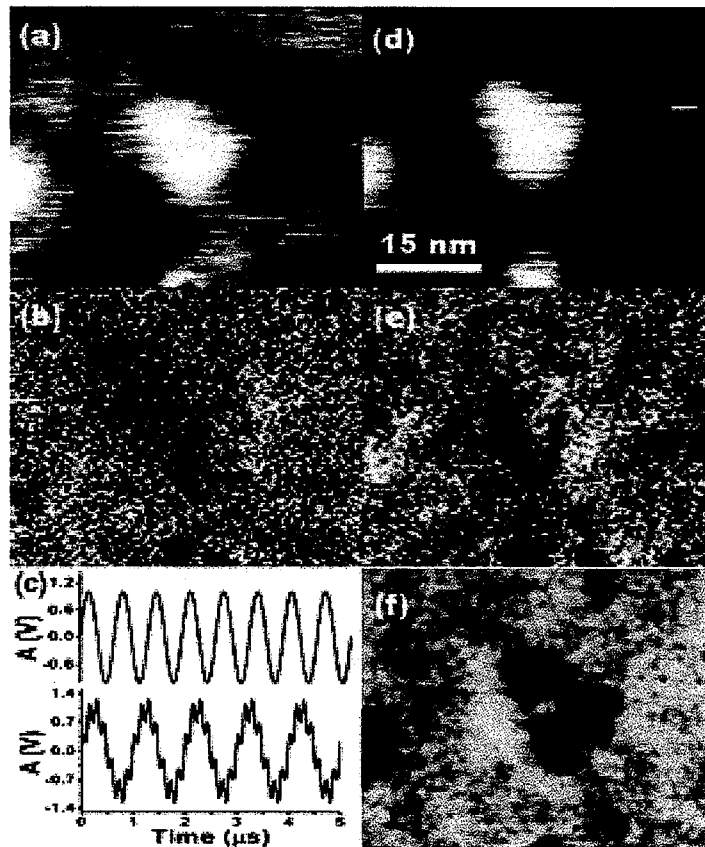


Figure 3. Comparison between AM-AFM and bimodal AFM images of IgG antibodies. (a) Topography and (b) phase images of an IgG obtained in AM-AFM. (c) Tip oscillation in AM-AFM (top) and bimodal AFM (bottom). (d) Topography in bimodal AFM. (e) Phase shift image of the first mode in bimodal AFM. (f) Bimodal AFM phase image (second mode) of the same antibody. The image shows a Y-shaped object.

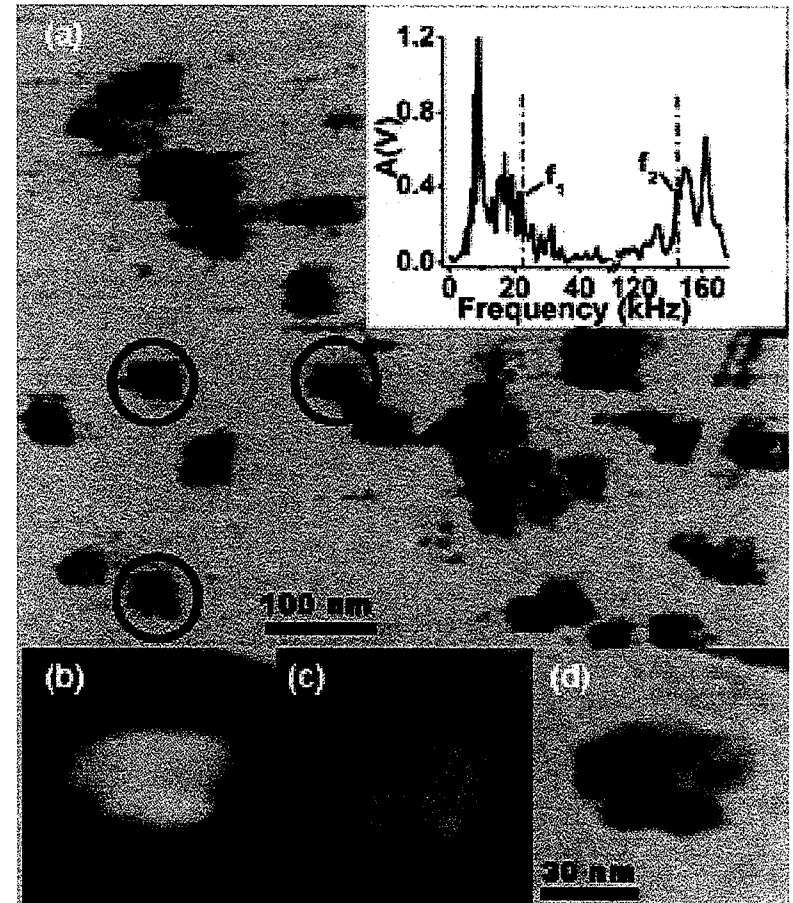


Figure 7. (a) Bimodal AFM phase images (second mode) of IgM antibodies in water. The objects that show a pentagonal shape are marked by circles. The inset shows the frequency spectrum of a commercial cantilever in water. The dashed lines indicate the frequencies of the first and second flexural modes of the cantilever. They were determined by measuring the thermal noise spectrum. (b) Topography of an isolated antibody. (c) First mode phase image and (d) bimodal AFM phase image (second mode) of the same antibody.

Multi-frequency AFM

■ Bimodal or dual AC

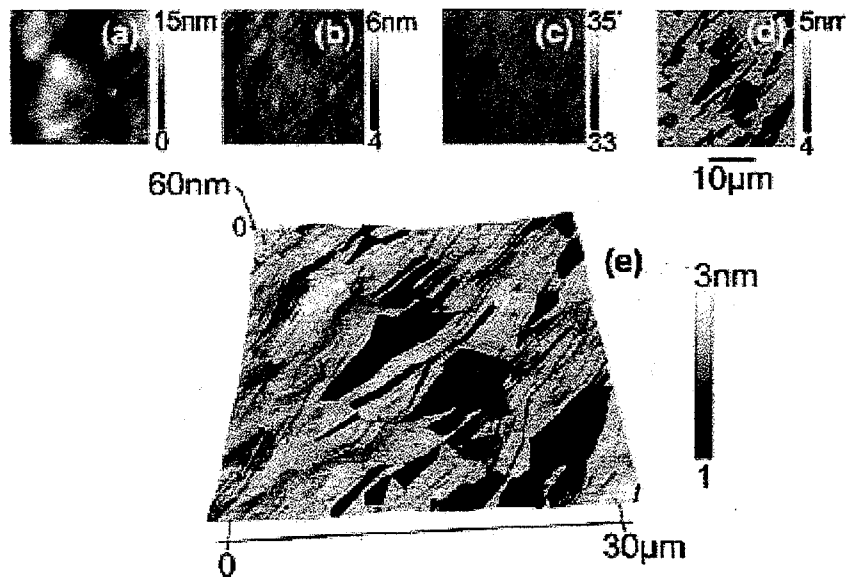


FIG. 2. (Color online) HOPG graphite surface, $30\ \mu\text{m}$ scan. The cantilever was driven at its fundamental ($\sim 69.5\ \text{kHz}$) and second eigenfrequency ($\sim 405\ \text{kHz}$). (a) shows the topography and (b) is the fundamental amplitude channel, used for the feedback error signal. The fundamental phase image (c) shows an average phase lag of $\sim 34^\circ$ indicating that the cantilever was in repulsive mode for the entire image. The second mode amplitude is shown in (d). The three dimensional rendered topography colored with the second mode amplitude is shown in (e). This method of display allows easy spatial correlation of the two channels.

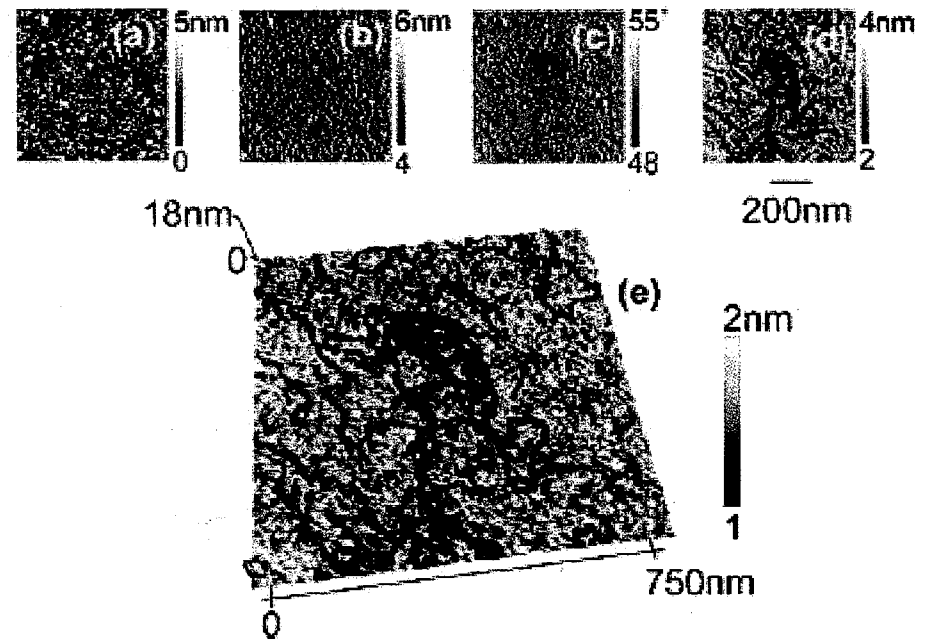


FIG. 3. (Color online) Dense mat of DNA imaged in buffer, $750\ \text{nm}$ scan. The $60\ \mu\text{m}$ Bio-Lever was driven at its fundamental resonance ($\sim 8.5\ \text{kHz}$) and at its second mode ($\sim 55\ \text{kHz}$). The topography (a), fundamental amplitude (b), and fundamental phase (c) all show very little differentiated contrast. The second mode amplitude (d) shows clear, high contrast images of what appear to be strands of DNA molecules. The second mode amplitude was painted onto the three dimensional rendered topography (e) to allow spatial correlation of the two data channels.

Other emerging dAFM techniques

- Multi-frequency AFM
- Sub-surface imaging
- High-speed/video rate AFM

Slide switch at ~46:00
Start ~50:30